Determination of the Electro-Optic Coefficient of β-BaB_2O_4 Crystal

Mehdi Keikha

Laser and Plasma Research Institute, Shahid Beheshti University, Tehran, Iran

Corresponding author email: mehdikeikha.op@gmail.com

Received: Mar. 08, 2025, Revised: July 05, 2025, Accepted: Sept. 07, 2025, Available Online: Sept. 09, 2025,
DOI: will be added soon

ABSTRACT— One of the most widely utilized physical properties in laser and photonic technologies is the electro-optic behavior of materials, characterized by their electro-optic coefficients. The electro-optic coefficient quantifies a material's ability to alter its optical properties in response to an applied electric field. When light passes through an electro-optic crystal subjected to an electric field, light modulation can be controlled with high speed and precision in accordance with the crystal's electro-optic coefficient. This property facilitates applications such as light control, frequency conversion, and the generation and amplification of short laser pulses. In this study, the electro-optic coefficient of the nonlinear beta barium borate (β-BaB_2O_4) crystal is determined by applying quarter-wave and half-wave voltages in an intensity modulator setup. It will also be demonstrated that this configuration serves as an effective method for the precise measurement of half-wave and quarter-wave voltages in Pockels cells.

KEYWORDS: Beta barium borate, Electro-optic Coefficient, Electro-optic modulators, Half-wave voltage, Intensity modulator, Pockels cell.

I. INTRODUCTION

Electro-optic Pockels cells are devices that utilize the birefringence property to modify light characteristics such as phase, amplitude, or polarization by applying an electric field to the electro-optic crystal contained within them [1]. The most commonly used crystals to date include KDP (Potassium Dihydrogen Phosphate), $LiNbO_3$ (Lithium Niobate), and BBO (Beta Barium Borate) [2]. Among the most significant applications of these crystals is the generation of high-power laser pulses, achieved through techniques such as Q-switching, mode-locking, and cavity dumping [3]. In most of these techniques, the switching operation is performed by rapidly turning the applied voltage to a Pockels cell on and off, functioning as an electro-optic shutter. The voltage required for switching depends on the crystal's biasing method, the crystal length, and its electro-optic coefficient [4]. Furthermore, the electro-optic coefficients of various crystals are influenced by the crystal type, composition, the doping level of different elements, and the growth method [5]. The BBO crystal (β-BaB_2O_4), due to its non-centrosymmetric structure, high thermal and dielectric damage thresholds, and a broad transparency range from 190 to 2500 nm, is an excellent choice for high-power applications as a Pockels cell [6]-[7]. Additionally, the electro-optic coefficient of this crystal is significantly smaller than that of KDP and $LiNbO_3$ crystals, making it more suitable for high-power applications compared to the other two crystals [8]. The configuration of a Pockels cell can be designed such that the electric field is applied either along the direction of the light beam propagation (longitudinal biasing) or perpendicular to the beam's propagation direction (transverse biasing). Due to the requirement of non-centrosymmetry in a specific direction of electro-optic crystals to induce birefringence from the Pockels effect, most KDP Pockels cells are longitudinally biased, while $LiNbO_3$ and BBO Pockels cells are transversely biased [9]. $LiNbO_3$ and BBO crystals possess trigonal

crystal structures and belong to the 3m point group, with their effective electro-optic coefficient for inducing the Pockels effect being r_{22} [1]. Various values for the electro-optic coefficients of these (bulk) crystals have been reported in the literature, typically determined by interferometric techniques such as Mach-Zehnder [10]-[11], Fabry-Perot [12]-[13] and Michelson interferometers [14]-[15] as well as by polarization modulation methods, particularly the Senarmont method [16]-[17]. Interferometric techniques are extensively employed for the precise measurement of electro-optic coefficients, particularly in crystalline materials. However, these methods require highly accurate optical alignment (to detect fringe displacement) and mechanical stability (to minimize fluctuations in the interferometer arms). They are extremely sensitive to mechanical vibrations, thermal fluctuations, and parasitic effects such as electrostriction and internal reflections within the sample, which can lead to systematic errors in the measurement results. Additionally, interferometers are vulnerable to phase instability and scattering in inhomogeneous or microscopically structured samples, resulting in reduced fringe contrast and diminished measurement accuracy. In contrast, the Senarmont compensator method, as a simple yet effective polarimetric technique, enables accurate determination of phase variation, refractive index modulation, and ultimately the electro-optic coefficient by employing polarized light in conjunction with a polarizer and an analyzer. This method operates based on the detection and rotation of polarization components by identifying the positions of minimum and maximum transmitted light intensity. As phase changes manifest as observable analyzer angle variations, the technique offers high sensitivity to optical birefringence. Due to its simplicity, reduced susceptibility to environmental noise, and minimal instrumentation requirements, the Senarmont method is considered a reliable and cost-effective option for both laboratory-scale investigations and educational applications [18],[19]. In this study, based on the second method, but using a simple setup, the intensity variations of a polarized beam (caused by polarization rotation due to an applied voltage) passing through an intensity modulator are measured. The electro-optic coefficient of the BBO crystal placed in the setup is then determined according to the amplitude of the applied voltage.

II. THEORY

As a light beam propagates through an anisotropic electro-optic crystal, it splits inside the crystal into two components or "modes" with orthogonal linear polarizations. Due to the anisotropic nature of the crystal, these two modes propagate with different velocities, $v_1 = c_0 / n_1$ and $v_2 = c_0 / n_2$ inside the material (where c_0 is the speed of light in vacuum and n_i is the refractive index of the material for that specific mode). Since the velocities are different, the two modes accumulate a relative phase difference after traveling a distance L through the crystal. This phase difference (or relative phase retardation), denoted by Γ, is given by:

$$\Gamma = k_0 \left[\Delta n\right] L \tag{1}$$

where k_0 is the propagation constant, $\Delta n = n_1 - n_2$ is the difference in refractive indices between the two modes, L is the length of the crystal along the light propagation direction. Now, if a static (DC) electric field is applied to the crystal, the refractive indices in different directions change due to a phenomenon called the Pockels effect. In other words, in the presence of an electric field, each refractive index n_i becomes $n_i(E)$, which depends on the amplitude of the electric field E [20]. The change in refractive index due to the Pockels effect is given by:

$$\Delta n\left(E\right) = r_{ij} E n_o^3 \tag{2}$$

In this equation n_o is the ordinary refractive index of the crystal (which varies depending on the wavelength passing through the crystal), and r_{ij} is the electro-optic coefficient of the crystal (which depends on the crystal type and

the field direction). If a transversely biased BBO (β-BaB_2O_4) crystal is employed, the most relevant component of the electro-optic tensor is r_{22} . In this case, the phase retardation between the two propagating waves (modes) is given by:

$$\Gamma = k_0 \left[r_{22} E n_o^3 \right] L \tag{3}$$

The relation between electric field and voltage is simply:

$$E = \frac{V}{d} \tag{4}$$

where V is the applied voltage across the crystal, and d is the distance between the two electrodes (i.e., the width of the crystal). From Eq. (3), the voltage required to produce a desired phase retardation Γ can be derived as follows:

$$V = \frac{\Gamma d}{k_0 \left[r_{22} n_o^3 \right] L} \tag{5}$$

For example, to generate phase shift of π or $\pi/2$ (i.e., $\Gamma = \pi$ or $\Gamma = \pi/2$), the required voltage corresponds to the so-called half-wave voltage $V_{\lambda/2}$ or quarter-wave voltage $V_{\lambda/4}$, respectively. The value of the ordinary refractive index of a BBO crystal for any specific incident wavelength can be determined using the following Sellmeier equation:

$$n_o = \sqrt{2.7359 + \frac{0.01878}{\lambda^2 - 0.01822} - 0.01354\lambda^2} \tag{6}$$

where λ the wavelength is expressed in micrometers [21]. By measuring the half-wave or quarter-wave voltage and knowing the crystal dimensions and the operating wavelength, the electro-optic coefficient r_{22} can be experimentally determined. One of the most accurate methods to measure the half-wave voltage is to use a setup in which a Pockels cell is placed between two crossed polarizers. If the Pockels cell introduces a phase retardation Γ and the polarizer transmission axes are oriented at 45° with respect to the crystal's principal axes (which rotate with applied voltage), the transmission ratio through this configuration follows the relation [20]:

$$T = \sin^2\left(\frac{\Gamma}{2}\right) \tag{7}$$

This equation can be derived using Jones matrices. The transmitted intensity can be easily controlled by adjusting Γ. This adjustment can be achieved, for instance, by deliberately altering the refractive indices via the application of an external DC electric field to the retarder. If the retarder is a Pockels cell, then Γ is linearly dependent on the applied voltage V (as described by Eq. (3) and Eq. (5)). Consequently, the transmission of this system exhibits a periodic dependence on V [22]:

$$T(V) = \sin^2\left(\frac{\pi}{2}\frac{V}{V_\pi}\right) \tag{8}$$

Here, V_π is the half-wave voltage ($V_\pi = V_{\lambda/2}$). When $V = V_\pi$, the induced phase shift is π. In this case, if the input light is linearly polarized at 45° with respect to the crystal axes, it will experience a 90° polarization rotation after passing through the crystal, becoming aligned with the second polarizer's transmission axis. Thus, the transmission coefficient of the system becomes 1, and the maximum light intensity is observed at the output of the modulator.

III. Experimental Setup

In this study, an intensity modulator setup, as shown in Fig. 1, was employed. This configuration consists of a BBO Pockels cell placed between two polarizers with orthogonal transmission axes.

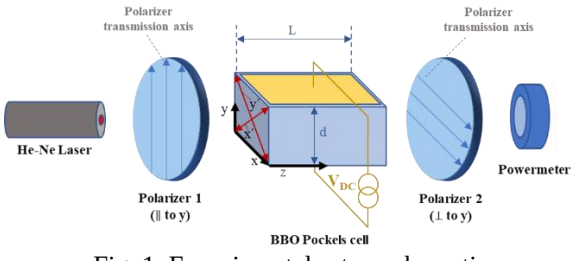

Fig. 1. Experimental setup schematic.

The transmission axis of Polarizer 1 was adjusted so that the incident laser beam on the crystal surface was polarized perpendicular to the plane of incidence (s-polarization). To align the transmission axis of Polarizer 2 orthogonally to that of Polarizer 1, the transmitted intensity through both polarizers was measured before inserting the Pockels cell into the setup. By rotating the transmission axis of the second polarizer to a specific angle, the transmitted intensity decreased to zero or reached its minimum. Under these conditions, Polarizer 2 was correctly aligned perpendicular to Polarizer 1. Once the polarizers were properly aligned, the BBO Pockels cell was inserted between them, ensuring it was aligned with the optical axis of the setup.

One of the most effective methods for aligning the electro-optic crystal in any optical setup is the "Maltese cross" interference pattern. When a light beam is incident on a birefringent crystal, it splits into two components: the ordinary ray (polarized along the optical axis) and the extraordinary ray (polarized perpendicular to the optical axis). When the Pockels cell is placed between two crossed polarizers, these components undergo different phase shifts. The relative phase difference between these components is $\Delta\Phi = 2\pi(n_e - n_o)/\lambda$ (where n_e and n_o are the extraordinary and ordinary refractive indices of the crystal, respectively). This phase difference leads to constructive interference (when $\Delta\Phi$ is an integer multiple of 2π) and destructive interference (when $\Delta\Phi$ is a half-integer multiple of 2π). Four dark regions appear along the arms of the cross due to destructive interference, while a central bright region completes the cross pattern due to constructive interference. As shown in Fig. 2, the optical axis of the crystal is precisely aligned with the optical axis of the setup when this interference pattern (cross shape) is completely symmetric. Under these conditions, the transmission efficiency of the modulator is optimized.

After preparing and aligning the experimental setup, the electrodes of the BBO Pockels cell were carefully connected to the high-voltage power supply (with caution to avoid disturbing the optical alignment that was achieved).

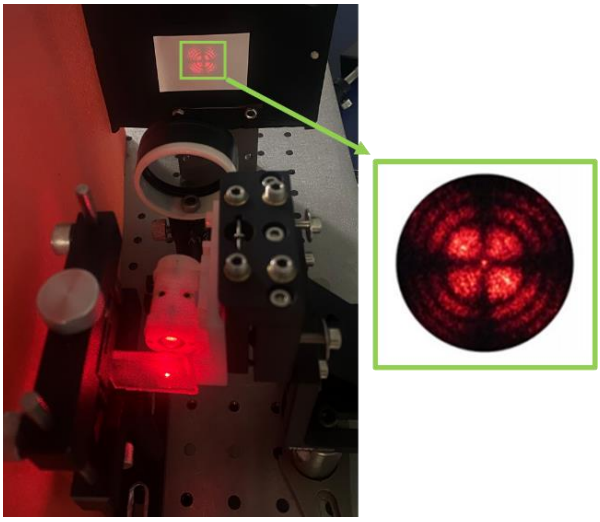

Fig. 2. The “Maltese Cross” interference pattern corresponding to two perpendicularly polarized components in a uniaxial crystal.

Subsequently, by applying voltage, variations in the transmitted optical power were measured using a power meter positioned at the output. In this experimental setup, an Ophir NOVA II handheld laser powermeter was used to measure the transmitted optical power. A BBPC4 model Pockels cell was used, incorporating a β-BaB_2O_4 (BBO) electro-optic crystal with physical dimensions of 4mm×4mm×30mm. The crystal is transversely biased within a cylindrical housing. In such transverse configurations, the electrodes (typically made of thin metallic layers such as gold or aluminum) are deposited directly onto the crystal's side surfaces, outside the optical path (in contrast to longitudinal bias configurations, where the electrodes are ring-shaped or transparent and placed near the input and output faces of the crystal). The use of metallic electrodes increases voltage tolerance and reduces electrical resistance, thereby enhancing modulation efficiency and overall stability of the system.

IV. Results

After preparing the experimental setup, the electrodes of the BBO Pockels cell were connected to a high-voltage power supply, and the voltage was increased in steps of 100V. To ensure voltage stability and accuracy, the

applied voltage was monitored both via the digital display of the power supply and independently verified using a high-voltage probe connected in parallel with the Pockels cell electrodes. At each voltage level, the optical power transmitted through the setup was measured using a calibrated digital power meter placed at the output end of the system. The device was configured to average the optical signal over a 1-second interval to suppress high-frequency noise and improve reading stability. For each voltage step, the transmitted power was monitored for approximately 10–20 seconds. During this interval, natural fluctuations in the transmitted optical intensity were observed, varying between a minimum and a maximum value. These fluctuations could originate from multiple factors, such as intrinsic laser power instability, ambient noise, the sensitivity and response time of the power meter, or, in some cases, non-uniformities in the electric field across the crystal due to imperfect electrode contact. The average of these fluctuating values was recorded as the representative data point for each voltage step in the transmission curve. Although a more accurate estimation of the standard deviation would require repeated measurements, it was approximated in this study as the range between the mean and the minimum or maximum power at each voltage level.

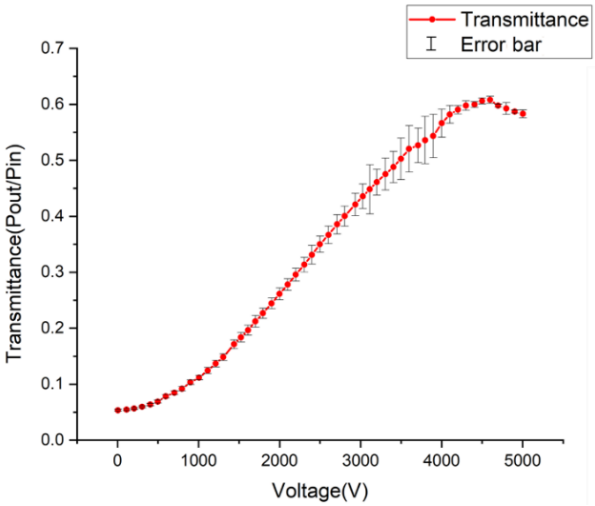

Fig. 3. Extraction of half-wave voltage from the modulator's transmission-voltage curve.

As shown in Fig. 3, the transmitted optical intensity reaches a maximum at approximately 4.55kV and then decreases. This voltage corresponds to the half-wave voltage (V_π) of the BBO crystal. At this voltage, the s-polarized incident beam passing through the crystal experiences a π phase retardation, effectively rotating its polarization by 90° and aligning it with the transmission axis of the second polarizer (as illustrated in Fig. 1). As a result, the transmitted optical intensity through the system reaches its peak. The BBO crystal used in this experiment has a thickness of $d = 4mm$ and a length of $L = 30mm$. Additionally, since the wavelength of the Helium-Neon laser used is 633nm, the ordinary refractive index of the crystal, according to Eq. (6), is $n_o = 1.6672$. Therefore, based on Eq. (5), the electro-optic coefficient of the BBO crystal is calculated to be $r_{22} \approx 2\,pm/V$. To validate this result, the experiment may be repeated under identical conditions. Furthermore, to reduce the required driving voltage and enhance reliability, a quarter-wave plate was inserted in the beam path after the Pockels cell, with its fast axis oriented at 45° with respect to the vertical plane of the optical table (as shown in Fig. 4).

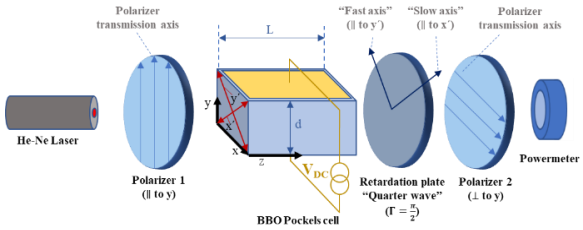

Fig. 4. Setup of Fig. 1 with an added quarter-wave plate for quarter-wave voltage measurement.

Under this configuration, the quarter-wave voltage applied to the crystal induces a phase shift of $\pi/2$ in the laser beam, while the quarter-wave plate contributes an additional $\pi/2$ phase shift. This combined effect produced the condition shown in Fig. 5, where the maximum transmitted intensity was observed at a voltage of 2.1kV. Since this value corresponds to half of the half-wave voltage amplitude, the electro-optic coefficient was calculated according to Eq. (5) to be $r_{22} \approx 2.2\,pm/V$.

As evident from the transmission curves in Figs. 3 and 5, the standard deviation and corresponding error bars (representing the

amplitude of optical power fluctuations at each voltage step) decrease significantly near the extrema (maxima and minima) of the curves.

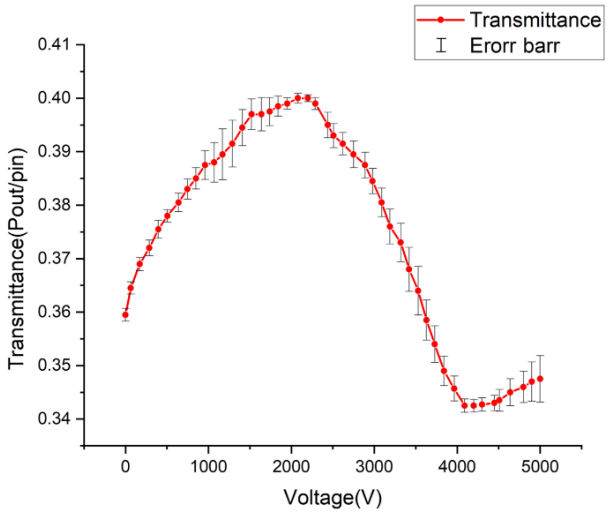

Fig. 5. Extraction of quarter-wave voltage from the modulator's transmission-voltage curve.

In Fig. 3, reduced fluctuations are observed at 0V and at the half-wave voltage (V_π), while in Fig. 5, similar stability appears at both the quarter-wave ($V_\pi/2$) and half-wave ($V\pi$) voltages. This behavior corresponds to the flatter slope of the transmission curve near its extrema, as expected from the sinusoidal voltage dependence described by Eq. (8). Differentiating both sides of this equation shows that the uncertainty in transmitted intensity (ΔI) is proportional to the derivative of intensity with respect to voltage (dI/dV), multiplied by the uncertainty in the applied voltage (ΔV). Assuming that voltage fluctuations are small and nearly constant, the reduced slope of the transmission curve at its maxima and minima leads to smaller variations in the output intensity, thereby reducing the measurement uncertainty in these regions.

V. Discussion

To assess the reliability of the measured electro-optic coefficient in this study, it is essential to compare the obtained values with those reported in previous works. Table 1 summarizes several experimentally determined values of the electro-optic coefficient r_{22} for β-BaB_2O_4 (BBO) crystals using different measurement techniques. In the present study, two independent measurements were performed (one based on half-wave voltage and the other using a quarter-wave configuration) and the electro-optic coefficient was calculated from each. The averaged result from both measurements yields $r_{22} \approx 2.1 \pm 0.1 pm/V$. This value closely agrees with those reported by Müller *et al.* [8] and Abarkan *et al.* [24], supporting the consistency and validity of the experimental approach based on intensity modulation. While this agreement affirms the accuracy of the method, it is still necessary to examine the causes of deviation between the experimental results and the theoretical predictions. Several physical and instrumental factors may affect the measured transmission, the applied voltages, and the extracted electro-optic coefficient. These influences are discussed in the following subsections, along with practical considerations for improving future experiments.

Table **1** Reported values of the electro-optic coefficient r_{22} for BBO crystals in various studies.

r_{22} reported (pm/V)	Measurement Method	Ref.
2, 2.2	Intensity modulator	Present work
2.5±0.1	Senarmont compensator	[23]
2.1, 2.2	Phase retardation , Mach-Zehnder interference	[8]
2.3±0.1 , 2.35±0.1	Michelson interference , Senarmont compensator	[15]
2.2±0.1	Senarmont compensator	[24]

A. *Comparison of Experimental Results with Theoretical Predictions*

Based on the obtained experimental data, the electro-optic coefficient was determined to be approximately $r_{22} \approx 2.1 \pm 0.1 pm/V$. By substituting this value, along with the predefined parameters, into Eq. (8), and plotting the transmission ratio numerically for both experimental setups, the resulting curves are shown in Fig. 6 (corresponding to Fig. 3) and Fig. 7 (corresponding to Fig. 5).

As shown in Figs. 6 and 7, the transmission of an ideal intensity modulator varies between a minimum of 0 and a maximum of 1. However, the experimental results deviated from this ideal behavior. In the setup without the quarter-wave

plate (Fig. 1), the transmission varied from 5% (minimum) to 63% (maximum). In the configuration with the quarter-wave plate (Fig. 4), the transmission ranged between 34.5% and 40%. These deviations result from various non-ideal optical and physical effects, which are analyzed in the following.

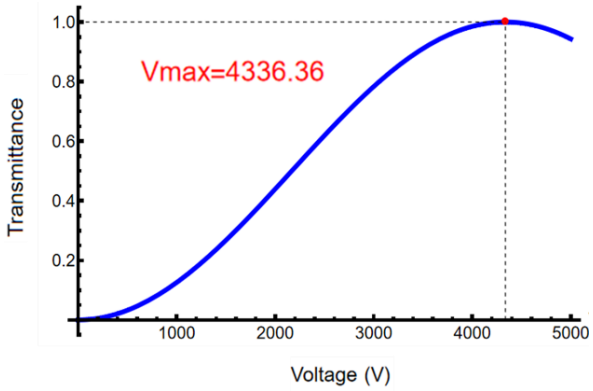

Fig. 6. Extraction the transmission ratio T(V) plot, defined by Eq. (8). To determine the half-wave voltage.

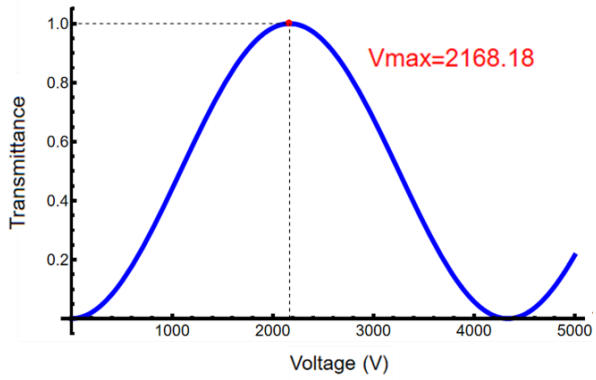

Fig. 7. Extraction the transmission ratio T(V'=2V) plot, defined by Eq. (8). To determine the quarter-wave voltage.

In the first setup (Fig. 1), when the applied voltage was zero, the input laser power was 2μW. After the first polarizer, the power dropped to 1.8μW, then to 1.53μW after the Pockels cell, and finally to 106nW after the second polarizer. The gradual decrease in power indicates that the input laser beam was not fully s-polarized, resulting in a 10% loss after the first polarizer. Moreover, due to the non-ideal extinction ratio of the crossed polarizers, approximately 5% transmission was observed when the Pockels cell was turned off. The Pockels cell also caused around 15% loss due to surface reflections (stemming from anti-reflection coatings optimized for a different wavelength), and due to internal scattering within the crystal. When the half-wave voltage ($V\pi$) was applied, the output power was measured to be 1.275μW, which is lower than the expected range of 1.8μW-2μW. This reduction in transmission from the ideal 100% to 63% is not only due to the loss at the first polarizer but also to the misalignment between the polarization direction of the incident beam and the voltage-induced x′ and y′ axes of the crystal (as shown in Fig. 1). According to our experimental observations, these combined effects result in a maximum transmission of approximately 63.75% and a minimum of 5.3% in this configuration.

In the second configuration (Fig. 4), which includes a quarter-wave plate, the transmission does not reach zero or one due to the intrinsic nature of circular polarization. At zero voltage, the quarter-wave plate converts the linear polarization of the input beam into circular polarization, ideally resulting in 50% transmission. However, the observed value was around 35%, primarily due to losses from the polarizers and the Pockels cell (consistent with the first configuration). When a voltage of V = Vπ/2 is applied, the Pockels cell introduces an additional π/2 phase shift, producing a total phase delay of π between orthogonal polarization components. This leads to a modest increase in transmission to about 40%, still lower than the 63% observed in the first setup. The reduced modulation depth (approximately 6% compared to 58%) is mainly attributed to the need for precise alignment of the quarter-wave plate's fast axis at 45 degrees with respect to the polarization direction entering the Pockels cell. As illustrated in Fig. 4, this alignment ensures proper polarization rotation to match the analyzer axis, a requirement that can be rigorously derived using Jones matrix formalism. Despite the lower modulation contrast in this setup, the primary goal of the experiment was to identify the transmission extrema (minimum and maximum values) needed for calculating the half-wave and quarter-wave voltages, and thereby determine the electro-optic coefficient. Measuring the full transmission range was not

the objective, although it remains useful for further system analysis.

B. *Applied Voltage Limitations and Optimization of V and $V_{\pi/2}$ Measurement Process*

As shown in Figs. 3 and 5, the applied voltage to the Pockels cell was limited to 5kV. This constraint results from the close spacing of the pins connected to the crystal electrodes, which are coupled to the power supply through high-voltage cables. Applying voltages beyond 5kV increases the risk of electrical discharge. To avoid such issues, the voltage applied to the crystal was restricted to a safe operational range. To enhance the accuracy of the $V\pi$ and $V_{\pi}/2$ determinations, the voltage step size can be reduced near the intensity maxima. This approach allows for more precise identification of the voltages corresponding to maximum transmission. It should also be noted that in practice, the required half-wave voltage may exceed the theoretical value. This discrepancy can arise from the non-uniformity of the electric field within the crystal, which is influenced by absorption and reflection at the electrode–crystal interface. Another important consideration during the experiment is ensuring the complete discharge of any residual charge stored in the Pockels cell. Since the cell behaves similarly to a capacitor (with a dielectric crystal between two electrodes), it can retain residual electric charges after each measurement. Therefore, it is essential to fully discharge the cell before each measurement step. Otherwise, unintended birefringence may occur even in the absence of an applied voltage, leading to deviations in the observed transmission.

C. *Theoretical Considerations Based on the Employed Crystal in the System*

Crystals are classified into seven crystal systems and 32 point groups according to their geometric symmetry. The Pockels effect occurs only in non-centrosymmetric crystals, since a center of symmetry precludes a linear electro-optic response. Among the 32 point groups, only 21 lack a center of symmetry and can exhibit the Pockels effect. Notable examples include the $\bar{4}3m$ (cubic), 6mm (hexagonal), $\bar{4}2m$ (tetragonal), 3m (trigonal), and m (monoclinic) groups. The effective electro-optic coefficient in a given crystal depends on the direction of the applied electric field, the light propagation direction, and the incident beam polarization. For instance, in a KDP crystal with symmetry group $\bar{4}2m$ under longitudinal biasing, the $r_{ij} = r_{63}$ component of the electro-optic tensor governs the induced birefringence. Thus, the type of crystal, the biasing configuration, and the electric field direction collectively determine the effective electro-optic coefficient in the Pockels effect.

Moreover, at low frequencies, the electric field can induce structural deformation via the piezoelectric effect, which modifies the refractive indices through the elasto-optic effect. This secondary contribution can be suppressed either by clamping the crystal or by applying a sufficiently high-frequency electric field that prevents mechanical deformation from following the field. In such cases, the electro-optic coefficients for free and clamped crystals are denoted as r_{Ik}^{T} and r_{Ik}^{S} respectively.

The BBPC4 Pockels cell used in this study features a robust, clamped housing and exhibits minimal piezoelectric ringing, indicating that the BBO crystal is effectively mechanically constrained. Therefore, the measured electro-optic coefficient corresponds to the clamped (or damped) value.

VI. Conclusion

The electro-optic coefficient of the β-BaB_2O_4 crystal was experimentally determined to be approximately $r_{22} \approx 2.1 \pm 0.1 pm/V$. Accurate determination of this coefficient is essential for assessing the performance of BBO in electro-optic applications such as intensity modulators, pulsed lasers, laser amplifiers, pulse pickers, and other related systems. Given the crystal's high damage threshold, broad transparency range, and strong nonlinear properties, precise knowledge of its electro-optic behavior is crucial for its proper selection and effective integration into photonic and laser systems.

REFERENCES

[1] F.A. López, J.M. Cabrera, and F.A. Rueda, "Bulk Electrooptic Applications," in Electrooptics, F.A. López, J.M. Cabrera, and F.A. Rueda, Eds., Boston, MA: Academic Press, ch. 7, pp. 193–218, 1994.

[2] R. Goldstein, "Pockels cell primer," Laser Focus, Vol. 34, no. 1, pp. 21-28, 1968.

[3] R.A. Kumar, "Borate crystals for nonlinear optical and laser applications: A review," J. Chem., Vol. 2013, Article ID 154862, 2013.

[4] M. Keikha, "Design and construction of Pockels cell driver to create adjustable delay with voltage in laser," M.S. thesis, Laser Research Institute, Shahid Beheshti Univ, Tehran, Iran, 2024.

[5] A. Ashkin, C. Boyd, and T. Dziedzic, "Photorefractive effect in crystals," Appl. Phys. Lett., Vol. 9, pp. 72-80, 1966.

[6] T.S.C. Chen, R. Li, Y. Wu, Z. Lin, Y. Mori, Z. Hu, J. Wang, S. Uda, M. Yoshimura, and Y. Kaneda, *Nonlinear Optical Borate Crystals*: *Principles and Applications*, New York, NY, USA: Springer, Ch. 6, pp. 343–376, 2012.

[7] D.N. Nikogosyan, "Beta barium borate (BBO)," Appl. Phys. A, Vol. 52, no. 6, pp. 359-368, Jun. 1991.

[8] C.T. Mueller, N.D. Duong, and P.M. Adams, "The electro-optic effect in beta barium borate," in Proc. LEOS Annu. Conf., 2–4 Nov. 1988, pp. 162–163.

[9] J. Salvestrini, M. Abarkan, and M. Fontana, "Comparative study of nonlinear crystals for electro-optic Q-switching of laser resonators," Opt. Mater., Vol. 26, no. 4, pp. 449–458, Sep. 2004.

[10] F.M. Shimizu and J.A. Giacometti, "Measurement of the electro-optic coefficient during the photoelectric-field assisted poling using a Mach-Zehnder interferometer," Rev. Sci. Instrum., Vol. 87, no. 12, pp. 123-456. 2016.

[11] K. Onuki, N. Uchida, and T. Saku, "Interferometric method for measuring electro-optic coefficients in crystals," J. Opt. Soc. Am., Vol. 62, no. 9, pp. 1030–1032, Sep. 1972.

[12] M. Jacques, F. Sandrine, S. Pierre, and G. Gregory, "Simultaneous determination of thermo- and electro-optic coefficients by Fabry-Pérot thermal scanning interferometry," in Proc. SPIE, Vol. 5252, pp. 423–430, 2004.

[13] C.A. Eldering, A. Knoesen, and S.T. Kowel, "Use of Fabry–Pérot devices for the characterization of polymeric electro-optic films," J. Appl. Phys., Vol. 69, no. 6, pp. 3676-3686, 1991.

[14] H.Y. Zhang, X.H. He, Y.H. Shih, and S.H. Tang, "A new method for measuring the electro-optic coefficients with higher sensitivity and higher accuracy," Opt. Commun., Vol. 86, no. 6, pp. 509–512, Dec. 1991.

[15] P. Ney, A. Maillard, M.D. Fontana, and K. Polgár, "Accurate interferometric method for the measurement of electro-optic coefficients: application to a single β-barium borate crystal," J. Opt. Soc. Am. B, Vol. 17, no. 7, pp. 1158-1165, Jul. 2000.

[16] L. Yang, L. Jun, Z. Zhongxiang, B. Amar, and G. Ruyan, "Optical and electro-optic properties of potassium lithium tantalate niobate single crystals," in Proc. SPIE, Vol. 8120, pp. 81201(1-8), 2011.

[17] L. Jin, K. Nara, K. Takizawa, and E. Kondoh, "Dispersion measurement of the electro-optic coefficient r_{22} of the $LiNbO_3$ crystal with Mueller matrix spectropolarimetry," Jpn. J. Appl. Phys., Vol. 54, no. 7, pp. 078003(1-3), Jul. 2015.

[18] A.V. Syuy and E.O. Kile, "Determination of electro-optic coefficients of lithium niobate crystal by polarization and interference methods," in Proc. SPIE, Vol. 10176, pp. 101761N(1-8), 2016.

[19] M. Aillerie, N. Théofanous, and M. D. Fontana, "Measurement of the electro-optic coefficients: description and comparison of the experimental techniques," Appl. Phys. B, Vol. 70, no. 3, pp. 317–334, Mar. 2000.

[20] B.E.A. Saleh and M.C. Teich, *Fundamentals of Photonics*. New York, NY, USA: Wiley, Ch. 21, pp. 980–983, 2019.

[21] V.G. Dmitriev, G.G. Gurzadyan, and D.N. *Nikogosyan, Handbook of Nonlinear Optical Crystals*. Berlin, Germany: Springer, pp. 96-102, 2013.

[22] S. . Wemple and M. DiDomenico, "Electrooptical and nonlinear optical properties of crystals," Appl. Solid State Sci., Vol. 3, pp. 367–369, 1972.

[23] C.A. Ebbers, "Linear electro-optic effect in β-BaB_2O_4," Appl. Phys. Lett., Vol. 52, no. 23, pp. 1948–1949, 1988.

[24] M. Abarkan, J.P. Salvestrini, M.D. Fontana, and M. Aillerie, "Frequency and wavelength dependences of electro-optic coefficients in inorganic crystals," Appl. Phys. B, Vol. 76, pp. 1–7, 2003.

Mehdi Keikha received his BSc in Optics and Laser Engineering from Shahid Bahonar University in 2021. He completed his MSc at the Femtosecond Lasers Research Laboratory, Shahid Beheshti University, from 2021 to 2024. His research interests include lasers, pulsed laser amplifiers, electronics, and nonlinear optics.